AIP | Applied Physics Letters

On the impact of indium distribution on the electronic properties in InGaN nanodisks

M. Benaissa, W. Sigle, T. K. Ng, R. El Bouayadi, P. A. van Aken, S. Jahangir, P. Bhattacharya, and B. S. Ooi

Citation: Applied Physics Letters **106**, 101910 (2015); doi: 10.1063/1.4915117
View online: http://dx.doi.org/10.1063/1.4915117
View Table of Contents: http://scitation.aip.org/content/aip/journal/apl/106/10?ver=pdfcov
Published by the AIP Publishing

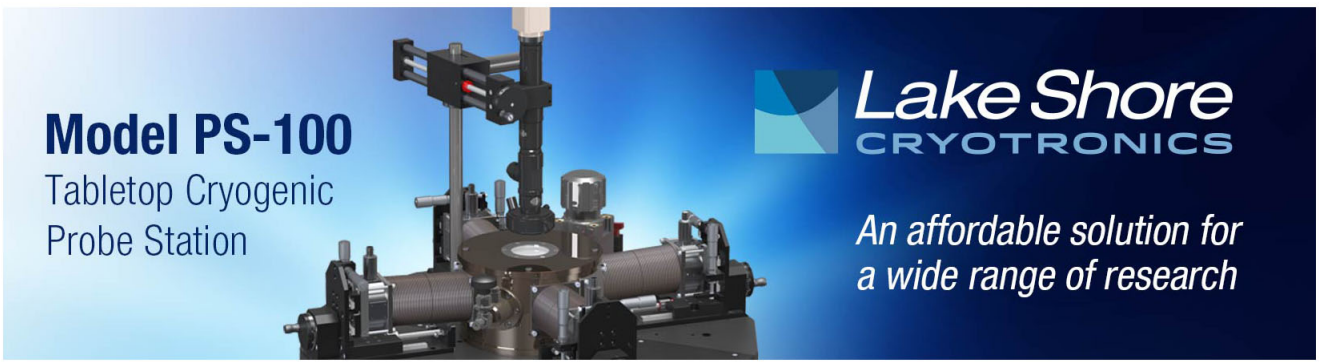

On the impact of indium distribution on the electronic properties in InGaN nanodisks

M. Benaissa,[1,a)] W. Sigle,[2] T. K. Ng,[3] R. El Bouayadi,[4] P. A. van Aken,[2] S. Jahangir,[5] P. Bhattacharya,[5] and B. S. Ooi[3]
[1]*LMPHE, Physics Department, Faculté des Sciences, Université Mohammed V, 4 Avenue Ibn Batouta, B.P. 1014 RP, 10000 Rabat, Morocco*
[2]*Max Planck Institute for Intelligent Systems, Heisenbergstraße 3, 70569 Stuttgart, Germany*
[3]*Photonics Laboratory, King Abdullah University of Science and Technology, Thuwal 23955-6900, Saudi Arabia*
[4]*LPMR, Université Mohammed Premier, B.P. 717, 60000 Oujda, Morocco*
[5]*Department of Electrical Engineering and Computer Science, University of Michigan, Ann Arbor, Michigan 48109-2122, USA*

(Received 25 November 2014; accepted 4 March 2015; published online 12 March 2015)

We analyze an epitaxially grown heterostructure composed of InGaN nanodisks inserted in GaN nanowires in order to relate indium concentration to the electronic properties. This study was achieved with spatially resolved low-loss electron energy-loss spectroscopy using monochromated electrons to probe optical excitations—plasmons—at nanometer scale. Our findings show that each nanowire has its own indium fluctuation and therefore its own average composition. Due to this indium distribution, a scatter is obtained in plasmon energies, and therefore in the optical dielectric function, of the nanowire ensemble. We suppose that these inhomogeneous electronic properties significantly alter band-to-band transitions and consequently induce emission broadening. In addition, the observation of tailing indium composition into the GaN barrier suggests a graded well-barrier interface leading to further inhomogeneous broadening of the electro-optical properties. An improvement in the indium incorporation during growth is therefore needed to narrow the emission linewidth of the presently studied heterostructures. © *2015 AIP Publishing LLC*.
[http://dx.doi.org/10.1063/1.4915117]

Due to their unique optoelectronic properties, InGaN/GaN quantum-well-based devices are increasingly used in a wide range of applications such as visible light-emitting diodes (LEDs)[1] and laser diodes.[2] Nowadays, however, self-organized semiconductor nanowires offer the possibility to grow heterostructures with negligible density of extended defects[3] and with a materials' combination that is difficult to achieve in the quantum-well configuration, particularly InGaN nanodisks (NDs) inserted in GaN nanowires.[4–6] In addition, InGaN/GaN nanowires exhibit very small piezoelectric fields[7] where the alloy composition in the nanodisks can be varied to tune the emission wavelength across the visible spectral range.[8]

To design InGaN/GaN nanodisks dedicated for light emitters with functionalities that are superior to those of current thin-film technologies, the InGaN nanodisks have to be quite narrow (around 3 nm) in order to obtain sufficient electron−hole overlap for polar heterostructures. Indium distribution among this multitude of nanodisks becomes therefore a serious challenge, since the emission from such a heterostructure will obviously produce a spectrum that encompasses a superposition of spectra from individual nanodisks. In such a complex system, any fluctuation of indium concentration, either within a given nanowire or from one nanowire to another, is expected to provoke differences in emission energy leading to a broad luminescence, usually characterized by a large full-width-at-half-maximum (FWHM) exceeding 400 meV.[9,10] Fluctuations in the form of bimodal[11] and gradient[12] indium distributions within individual nanowires were indeed reported, but the impact of such non-homogeneities on the electronic properties, and thus on the optical properties, need additional careful studies.

To truly shed light on the electronic properties of these individual InGaN nanodisks and therefore on the origin of the emission broadening, a spatial resolution superior to the nanodisk dimension is needed. Optical techniques traditionally used for bandgap determination have excellent energy resolution (down to the meV range) but are limited in achieving nanoscale measurements due to their micron-range spatial resolution. However, low-loss electron energy-loss spectroscopy (low-loss EELS) performed in a modern transmission electron microscope (TEM) is an unrivaled tool to probe electronic properties at the nanodisk scale. In the present study, a modern TEM equipped with a monochromated electron probe, small as a few angstroms, is used to perform low-loss EELS combined with energy-filtering TEM (EFTEM) imaging to retrieve valuable information on the indium content distribution, on one hand, and its impact on the electronic properties of individual nanodisks, on the other.

InGaN/GaN nanowire heterostructure can be grown on (001)- and (111)-oriented Si substrates.[13] In the present study, catalyst-free GaN nanowires were grown on Si-(111) substrate by molecular beam epitaxy (MBE). Six 3-nm sized InGaN nanodisks were vertically incorporated and stacked in

a)Author to whom correspondence should be addressed. Electronic addresses: benaissa.um5@gmail.com and benaissa@fsr.ac.ma

each GaN nanowire, but separated by a 12-nm GaN barrier. The disk height and the barrier thickness were controlled by the growth time. More details on the growth process can be found elsewhere.[14] Fig. 1(a) shows a top-view scanning electron microscopy (SEM) image of the InGaN/GaN nanodisk heterostructures. The as-imaged nanowires exhibit a hexagonal shape with vertical faceted sidewalls (see inset in Fig. 1(a)). The areal density of the nanowires is estimated around $6 \times 10^{10}\,\mathrm{cm}^{-2}$ with a fair degree of size uniformity. A nanowire lateral width of about 50 nm can be measured. A side-view bright-field TEM image of these free-standing InGaN/GaN nanodisk heterostructures is shown in Fig. 1(b), exhibiting an average length of 200 ± 26 nm. The wires are vertically aligned, with the *c*-axis lying along the growth direction normal to the substrate.

In order to gain a quantitative examination of indium content, high-angle annular-dark-field (HAADF) imaging is performed on a single nanowire as shown in Fig. 2(a). A collection angle greater than 55 mrad was used to obtain a contrast that is strongly dependent on the atomic number *Z* of the existing elements: the higher the atomic number, the brighter the HAADF image intensity. In Fig. 2(a), this change in contrast is clearly highlighted where the InGaN nanodisks look brighter, since the average atomic number in the nanodisk region is larger than that in GaN barriers. However, an analysis of the HAADF intensities, using an integrated line profile, shows that the amplitude of the intensities is not uniform (see Fig. 2(b)). Strikingly, the profiles do not clearly reveal the nominal nanodisk width of 3 nm but appear wider. This indicates interdiffusion among the InGaN and GaN layers. In order to extract the indium concentration from this line profile, we used a calibration curve. We simulated the HAADF contrast intensity using a model composed of an InGaN nanodisk (3 nm in height) sandwiched between two GaN barriers (see inset up-right in Fig. 2(c)), where the indium content of the nanodisk is varied from 0% to 100%. The HAADF simulation procedure is reported elsewhere.[15] For each indium concentration, [In], the ratio $\frac{I^{\mathrm{InGaN}}_{\mathrm{HAADF}}}{I^{\mathrm{GaN}}_{\mathrm{HAADF}}}$ is calculated, where $I^{\mathrm{InGaN}}_{\mathrm{HAADF}}$ and $I^{\mathrm{GaN}}_{\mathrm{HAADF}}$ correspond to simulated HAADF intensities of InGaN and GaN, respectively. This ratio is then drawn as a function of [In] (see bottom-left of Fig. 2(c)). In order to extract indium concentrations from the experimental HAADF data shown in Fig. 2(a), the same ratio was deduced where the HAADF intensity of the GaN base-part is used as the experimental $I^{\mathrm{GaN}}_{\mathrm{HAADF}}$. The quantified indium concentration profile across the six InGaN nanodisks (see Fig. 2(c)) shows a variation from 10 to 20 at. % along the six nanodisks (indicated as ND1 to ND6). Such an indium distribution may explain the broadening observed in luminescence.

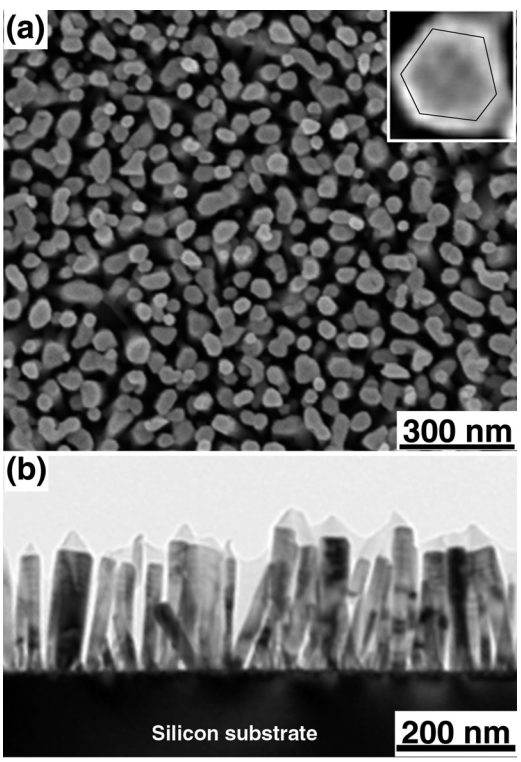

FIG. 1. (a) Top-view SEM image of InGaN nanodisks inserted in GaN nanowires. The inset (top-right) exhibits the hexagonal shape of the nanowires with vertical faceted sidewalls. (b) Side-view TEM image of the heterostructure. The wires are vertically aligned, with the *c*-axis lying perpendicular to the substrate.

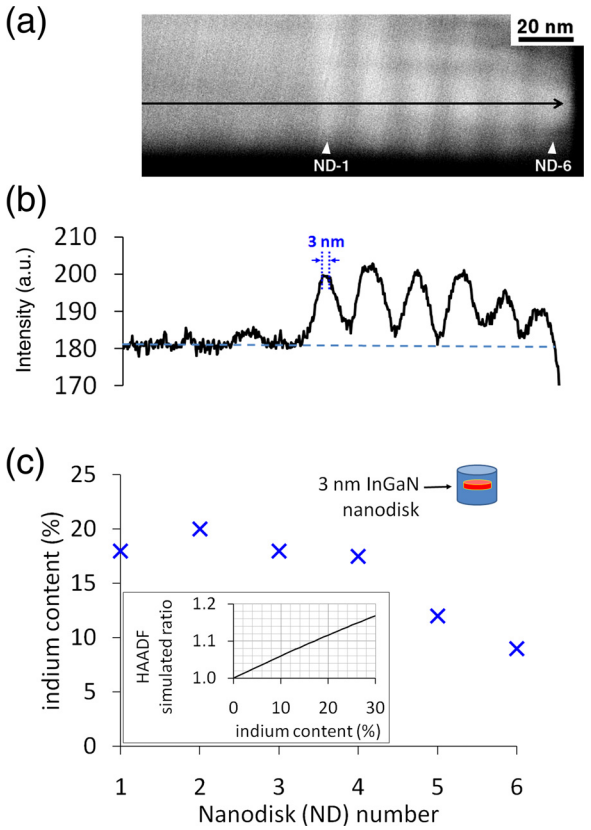

FIG. 2. (a) HAADF image of a single InGaN/GaN nanowire where InGaN NDs have a pronounced bright contrast, marked by white arrows. (b) The integrated line profile (indicated in (a) as a dark arrow) shows irregularities in the intensity amplitude. (c) Indium content profile (crosses) as a function of the nanodisk number as extracted from the line profile in (b). The model used is illustrated top-right. The calibration curve $\frac{I^{\mathrm{InGaN}}_{\mathrm{HAADF}}}{I^{\mathrm{GaN}}_{\mathrm{HAADF}}}$ ratio as a function of indium concentration is shown bottom-left.

Because this kind of In distribution should have an impact also on the dielectric properties, we thus explore the dielectric response of the above studied nanowire using low-loss EELS, in particular, collective excitations of charge carriers, so-called plasmons.[16] We take advantage of the

excellent isochromaticity and high transmissivity of the MANDOLINE in-column filter to map plasmon energies (<50 eV) at high energy resolution across a wide field of view. Owing to the electron monochromator, the energy resolution of the Zeiss SESAM[17] microscope is around 80 meV.[18] A series of energy-filtered images was acquired at energy losses from 17 to 26 eV using a 0.23-eV energy-selecting slit and energy-loss increments of 0.3 eV. From the image series, the plasmon energy is determined via a Gaussian fit to the plasmon peak.[19] The resulting plasmon-energy map is shown in Fig. 3(a) on the same nanowire as above. An integrated line profile across the plasmon-energy map is displayed in Fig. 3(b). One can see sinusoidal variation across the multilayer region. The energy maxima correspond to the GaN regions, whereas energy minima correspond to InGaN which is known to have lower plasmon energy (E_p)-values than pure GaN.[20] Note that the maxima corresponding to GaN are shifted towards lower energy with respect to those of the GaN-basepart. This shift is most likely caused by the In penetration into the GaN layers suggesting a graded composition well-barrier and therefore an inhomogeneous broadening of the resulting electro-optical properties, consistent with the results from HAADF intensities (other effects leading to plasmon energy shifts, as mentioned later, are negligible here because the GaN layers are relatively thick). The GaN plasmon energies are fairly constant, whereas the InGaN plasmon energies fluctuate considerably. In order to depict an overview picture of these indium fluctuations across nanodisks, E_p values from 4 nanowires (i.e., from 24 InGaN nanodisks) were extracted from our EFTEM images, as illustrated in Fig. 4(a). Apparently, each nanowire seems to have its own indium fluctuation and therefore its own average composition. These E_p values were then regrouped and presented as a statistical distribution illustrated in Fig. 4(b) in order to show how frequent certain plasmon energies are detected. This distribution is fitted with a Gaussian curve the FWHM of which is determined to approximately 600 meV centered on 19.2 eV, reflecting consequently the occurrence of a significant spread in indium concentration. This spread of plasmon energy values reflects a scatter in the complex optical dielectric function. Such a distribution readily accounts for the contribution to the origin of the luminescence spectral width, where the band structure will inevitably be characterized by an alteration in the vicinity of direct band-to-band transitions, despite the fact that the carriers are deeply localized in InGaN nanodisks and their migration is hindered.

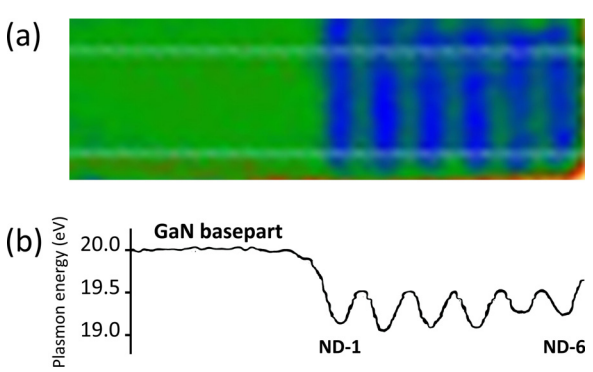

FIG. 3. (a) EFTEM image of the same nanowire as in Fig. 2. An integrated line profile across this image is shown in (b).

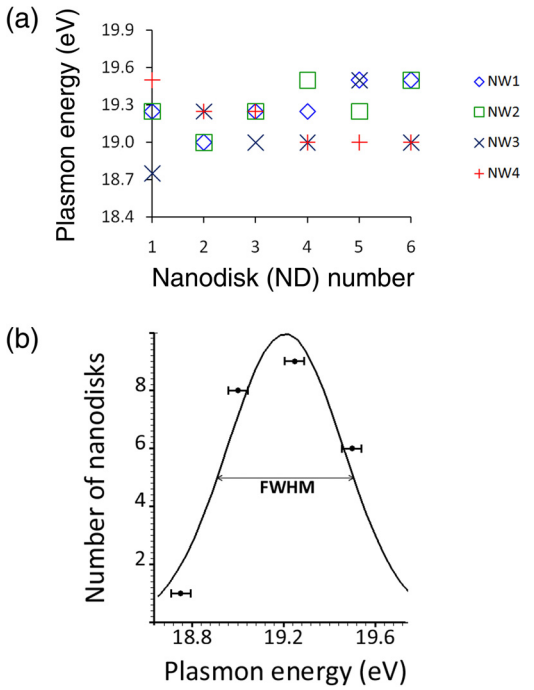

FIG. 4. (a) Plasmon energy values from 4 nanowires (NW1-NW4), that is 24 InGaN nanodisks, as extracted from EFTEM images. (b) Histogram showing the frequency of E_p values. From a fit to a Gaussian distribution, the FWHM is determined to approximately 600 meV centered on 19.2 eV. The error bar is around 80 meV.

Finally, it is worth mentioning that in the particular case of a 3-nm wide InGaN disk inserted in a GaN nanowire, nanoscale low-loss EELS measurements are known to be affected by intrinsic factors[21] such as interfaces, strain, and confinement. The interface contribution comes from the "begrenzungs" effect[22] induced by the closeness of the InGaN/GaN interfaces, that of strain comes from the fact that the fully strained 3-nm sized InGaN nanodisk on a relaxed GaN causes a shrinkage of the unit cell volume that is inversely proportional to the plasmon energy square,[23] while the confinement contribution is known to be inversely proportional to the nanodisk's size squared.[24] All these effects will tend to shift the InGaN plasmon energy peak to higher energies, a shift that should anyway be deducted from the as-measured values. The determination of these effects is not relevant for the present study and will depend on the nanodisk composition. However, each measured plasmon-energy encompasses *a fortiori* contributions from all those factors. We then conclude that the observed plasmon-energy distribution broadening, e.g., 600 meV, has globally its origin in the varying chemical composition, in accordance with our HAADF results, and can be correlated to the 400 meV luminescence broadening using the Penn model[25] for the dielectric function of a semiconductor.

In summary, we have employed monochromated low-loss EFTEM imaging to evaluate the electronic properties variation among InGaN nanodisks inserted in GaN nanowires. Using this powerful electron-based optical technique, we have demonstrated that each nanowire has its own indium fluctuation and therefore its own average composition. This

variety of indium averages was found to cause a scatter in plasmon energies, and therefore, in the dielectric function of the nanowires ensemble that will significantly alter band-to-band transitions. The latter will obviously induce an emission broadening that can probably be sharpened through enhanced indium incorporation during growth. More attention must then be given to growth conditions in order to help the emergence of optoelectronic devices that feature better performance, low cost, and low-power consumption.

The research leading to these results has received funding from the European Union Seventh Framework Programme [FP7/2007-2013] under Grant Agreement No. 312483 (ESTEEM2). U. Salzberger (from MPI-IS, StEM) is particularly acknowledged for her technical help in TEM sample preparation. T. K. Ng gratefully acknowledges financial support from KAUST baseline funding and Competitive Research Grant.

[1]S. Nakamura, Science **281**, 956 (1998).
[2]S. Nakamura, M. Senoh, S. Nagahama, N. Iwasa, T. Yamada, T. Matsushita, H. Kiyoku, and Y. Sugimoto, Jpn. J. Appl. Phys., Part 2 **35**(1B), L74 (1996).
[3]S. F. Garrido, J. Grandal, E. Calleja, M. A. S. Garcia, and D. L. Romero, J. Appl. Phys. **106**, 126102 (2009).
[4]S. Jahangir, M. Mandl, M. Strassburg, and P. Bhattacharya, Appl. Phys. Lett. **102**, 071101 (2013).
[5]S. Deshpande, J. Heo, A. Das, and P. Bhattacharya, Nat. Commun. **4**, 1675 (2013).
[6]W. Guo, A. Banerjee, P. Bhattacharya, and B. S. Ooi, Appl. Phys. Lett. **98**, 193102 (2011).
[7]W. Guo, M. Zhang, A. Banerjee, and P. Bhattacharya, Nano Lett. **10**, 3355 (2010).
[8]H. P. T. Nguyen, K. Cui, S. Zhang, S. Fathololoumi, and Z. Mi, Nanotechnology **22**, 445202 (2011).
[9]Y. Kamali, B. R. Walsh, J. Mooney, H. Nguyen, C. Brosseau, R. Leonelli, Z. Mi, and P. Kambhampati, J. Appl. Phys. **114**, 164305 (2013).
[10]M. Wölz, J. Lähnemann, O. Brandt, V. M. Kaganer, M. Ramsteiner, C. Pfüller, C. Hauswald, C. N. Huang, L. Geelhaar, and H. Riechert, Nanotechnology **23**, 455203 (2012).
[11]M. Knelangen, M. Hanke, E. Luna, L. Schrottke, O. Brandt, and A. Trampert, Nanotechnology **22**, 365703 (2011).
[12]G. Tourbot, C. Bougerol, F. Glas, L. F. Zagonel, Z. Mahfoud, S. Meuret, P. Gilet, M. Kociak, B. Gayral, and B. Daudin, Nanotechnology **23**, 135703 (2012).
[13]T. Frost, S. Jahangir, E. Stark, S. Deshpande, A. Hazari, C. Zhao, B. S. Ooi, and P. Bhattacharya, Nano Lett. **14**, 4535 (2014).
[14]S. Jahangir, T. Schimpke, M. Strassburg, K. A. Grossklaus, J. M. Millunchick, and P. Bhattacharya, IEEE J. Quantum Electron. **50**(7), 530 (2014).
[15]R. ElBouayadi, M. Korytov, P. A. van Aken, P. Vennéguès, and M. Benaissa, Phys. Status Solidi C **11**, 284 (2014).
[16]H. Raether, *Excitations of Plasmons and Interband Transitions by Electrons* (Springer, Berlin, 1980).
[17]C. T. Koch, W. Sigle, R. Höschen, M. Rühle, E. Essers, G. Benner, and M. Matijevic, Microsc. Microanal. **12**, 506 (2006).
[18]C. T. Koch, W. Sigle, J. Nelayah, L. Gu, V. Srot, and P. A. van Aken, *in* 14th European Microscopy Congress: *Instrumentation and Methods*, edited by M. Luysberg, K. Tillmann, and T. Weirich (Springer-Verlag, Berlin, Heidelberg, 2008), Vol. 1, pp. 447–448.
[19]W. Sigle, S. Krämer, V. Varshney, A. Zern, U. Eigenthaler, and M. Rühle, Ultramicroscopy **96**, 565 (2003).
[20]X. Kong, S. Albert, A. Bengoechea-Encabo, M. A. Sanchez-Garcia, E. Calleja, and A. Trampert, Nanotechnology **23**, 485701 (2012).
[21]M. Benaissa, W. Sigle, M. Korytov, J. Brault, P. Vennéguès, and P. A. van Aken, Appl. Phys. Lett. **103**, 021901 (2013).
[22]A. Howie, Ultramicroscopy **11**, 141 (1983).
[23]P. Drude, Phys. Z. **14**, 161 (1900).
[24]M. Mitome, Y. Yamazaki, H. Takagi, and T. Nakagiri, J. Appl. Phys. **72**, 812 (1992).
[25]D. R. Penn, Phys. Rev. **128**, 2093 (1962).